



## Quantum Mechanical Calculations of Photovoltaic and Photoelectronic Properties of Oligoselenophene/Fullerene BHJ Solar Cells

Z. Mahdavifar\*, S. Tajdinin and E. Shakerzadeh

Department of Chemistry, Faculty of Science, Shahid Chamran University of Ahvaz, Ahvaz, Iran

(Received 18 June 2020, Accepted 16 July 2020)

To model the active layer in the hetero-junction solar cells, the  $C_{60}$ ,  $C_{70}$ ,  $PC_{60}BM$ ,  $PCBDAN$  fullerenes as acceptor, and  $(OS)_{n=1}$  oligoselenophenes as donor were considered. The  $(OS)_{n=14}/C_{60}$ ,  $(OS)_{n=14}/C_{70}$ ,  $(OS)_{n=14}/PC_{60}BM$  and  $(OS)_{n=14}/PCBDAN$  blends as a model of the active layer in the BHJ solar cell were chosen, and the optoelectronic properties were studied. The calculated efficiency of these complexes based on the Scharber diagram is 8%, 8.2%, 9.3% and 9.7%, respectively. These results indicate that the  $(OS)_{n=14}/PCBDAN$  blend is a favorable candidate as solar cell than that of the other blends. In order to investigate the effect of the chain length of oligomers on the solar cell properties, the optoelectronic properties of  $(OS)_{n=12}/C_{60}$  blend was also studied. The electronic and optical properties and the calculated efficiency values of  $(OS)_{n=12}/C_{60}$  and  $(OS)_{n=14}/C_{60}$  (7.7% and 8% respectively) show that the  $(OS)_{n=14}/C_{60}$  complex is more suitable candidate than the  $(OS)_{n=12}/C_{60}$  complex for modeling the active layer in the BHJ solar cells.

**Keywords:** Oligoselenophene, Fullerene, Hetro-junction solar cell, DFT

### INTRODUCTION

Nowadays, because of fossil fuels declining and the environmental damage, clean and renewable solar energy as an inexhaustible resource has attracted increasing attention over the past decades due to nontoxic and nonpolluting operation [1]. The annual solar radiation coming to earth (including 5% UV, 43% visible and 52% IR) is several times the world's annual energy consumption [2]. In this context, organic photovoltaic (OPV) devices have attracted much attention in recent years [3,4,5,6,7]. There are many reasons for the interest in OPVs comparing with silicon-based photovoltaics (PV). The OPVs offer low cost, solution-based processing, low thermal budget, and the capability to fabricate flexible layer-area devices [3,8]. Organic photovoltaics are devices that convert solar energy or light directly into electrical power by photovoltaic effect [9]. The photovoltaic effect describes the fundamental

interaction of light with matter to produce electricity. Light with photon energy more significant than the band gap is absorbed by a semiconductor material [9,10]. Organic solar cells mainly consist of two organic materials, one of which is an electron donor (D) materials, and other is an electron acceptor (A) material [11]. An organic photovoltaic cell is composed of a film of the organic photovoltaic active layer, sandwiched between a transparent electrode and a metal electrode. Chemically, such devices usually consist of conjugated polymers (as electron donor) and fullerene derivatives (as an electron acceptor) [12-14].

Among organic semiconducting materials implemented into organic photovoltaics, the bulk heterojunction (BHJ) approach formed by blending donor type conjugated polymers with acceptors like fullerenes, has been the most attractive and successful one. Solution-processed bulk-heterojunction [15,16] photovoltaic cells were first reported in 1995 [17,18]. Bulk heterojunction polymer solar cells based on conjugated polymer donors (p-type) and functionalized fullerene acceptors (n-type) is a new and

\*Corresponding author. E-mail: [z\\_mahdavifar@scu.ac.ir](mailto:z_mahdavifar@scu.ac.ir)

expanding research field [19,20]. Therefore, this approach improves the power conversion efficiency of the OPV devices up to the 6-7% power conversion of efficient (PEC) plastic solar cell [21-23]. Various materials have been designed and synthesized to achieve high solar cell performance [14,17,24-27].

Several factors influence the performance of the solar cell. To increasing the solar cell performance, broad absorption bands, and appropriate molecular energy levels of the polymer are first required, therefore, finding the efficient way to lower the band gap of conjugated polymer is crucial the molecular design of the polymer. For the electron donor materials, one of the most important properties is a strong absorption covering a broad spectral region, whereas the band gap is less than 2 eV [3,5,28-30]. Low band gap (LBG) polymers show a promising to increase the power conversion efficiency (PEC) of BHJ [19]. One of the strategies to design low band gap (LBG) polymers is building a conjugated structure with alternative electron donor and electron acceptor units (D/A structure) that is an effective approach to get LBG polymer [31-36].

Thiophene-based conjugated polymers are conventionally applied in the optoelectronic devices due to the promising properties [37,38]. The outstanding properties of thiophene-based materials suggest that heterocyclic analogues, such as furan [39], polyselenophene [40] and tellurophene-based materials [41,42] should become an important member of the conduction polymer family and hope that these materials would suggestion interesting new electro-optical properties.

Selenium with atomic number 34 is similar to sulfur in many properties of thiophene and selenophene rings. Selenophenes are thought to compensate for some of the disadvantages of thiophene containing compounds. The possible advantages of ployselenophenes are anticipated to result from the unique properties of the Se atom namely the size of the selenium atom is bigger than that of sulfur and the electronegativity of selenium is weaker than that of sulfur [37,38]. In general, selenophene containing compounds have the advantages of lower oxidation and reduction potentials, strong light absorptivity, ease of polarizability, and improved inter-chain charge transfer, while maintaining structural similarities to thiophenes. Hence, it motivated us to investigate the opto-electronic

properties of ployselenophenes as donor materials in BHJ solar cell [43,44].

## COMPUTATIONAL DETAILS

Quantum-chemical calculations by density functional theory (DFT) using the Gaussian 09 programs [45] were performed to investigate the electronic structure of these (OS)<sub>n</sub>/fullerene blends by employing the B3LYP hybrid density functional. The basis sets used for the calculations are the split valence 6-311G(d) basis set. The B3LYP/6-311G(d) and CAM-B3LYP/6-311G(d) level of theories were applied to ensure the accuracy of the results. Obtained data indicated that the long-range corrected CAM-B3LYP functional was not adequate to predict the electronic properties in accordance with the experimental data [46]. Consequently, the B3LYP/6-311G(d) was utilized as a calculation method since computation at this level of theory has been shown to give accurate results, from the geometry and electronic evaluation points of view. Time-dependent TD-DFT (TD-DFT) [47,48] calculations were performed to assess the excited-state vertical transition energies and oscillator strengths based on the optimized molecular geometries at the same level of theory. To investigate the optoelectronic properties, the first 30 singlet-singlet excited states were calculated based on the optimized geometry at the same level of theory.

## RESULTS AND DISCUSSION

### Ground-State Properties

The optimized geometry of all studied complexes was shown in Figs. 1 and 2. On the basis of the optimized ground-state geometries of (OS)<sub>n=14</sub>/PCBDAN, (OS)<sub>n=14</sub>/PC<sub>60</sub>BM, (OS)<sub>n=12</sub>/C<sub>60</sub>, (OS)<sub>n=14</sub>/C<sub>70</sub> and (OS)<sub>n=14</sub>/C<sub>60</sub> complex, the deformation energy ( $E_{\text{def}}$ ), interaction energy ( $E_{\text{int}}$ ), adsorption energy ( $E_{\text{add}}$ ) were calculated and are presented in Table 1. Before investigating the electronic properties of formed complexes, we first need to validate their stability and ease of experimental synthesis. In order to further understand the stability of the formed BHJ blends, the adsorption energy, interaction energy as well as deformation energies were calculated using the following equations:

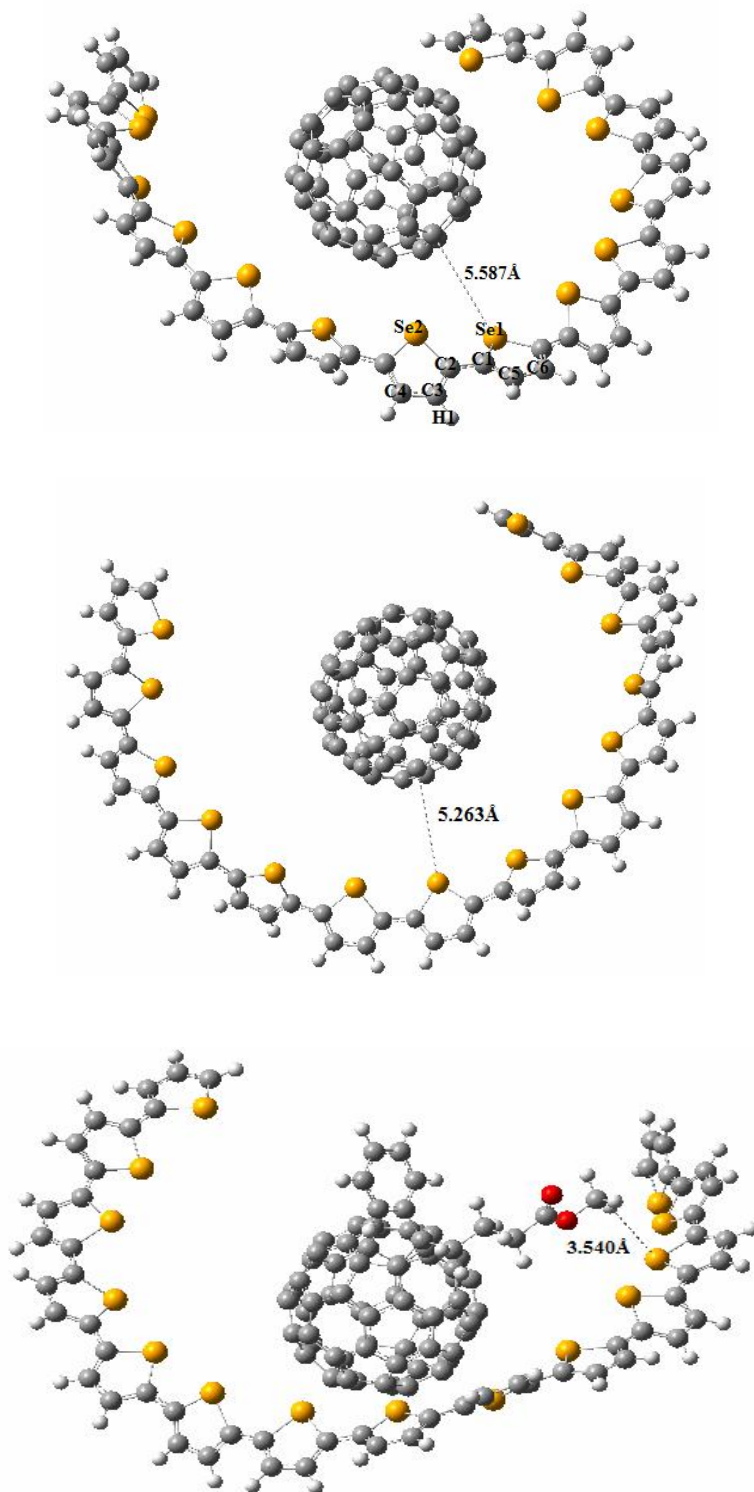


**Fig. 1.** Optimized geometries of (OS)<sub>n=14</sub>/PCBDAN, (OS)<sub>n=14</sub>/PC<sub>60</sub>BM, (OS)<sub>n=12</sub>/C<sub>60</sub>, (OS)<sub>n=14</sub>/C<sub>70</sub>, (OS)<sub>n=14</sub>/C<sub>60</sub> blends.

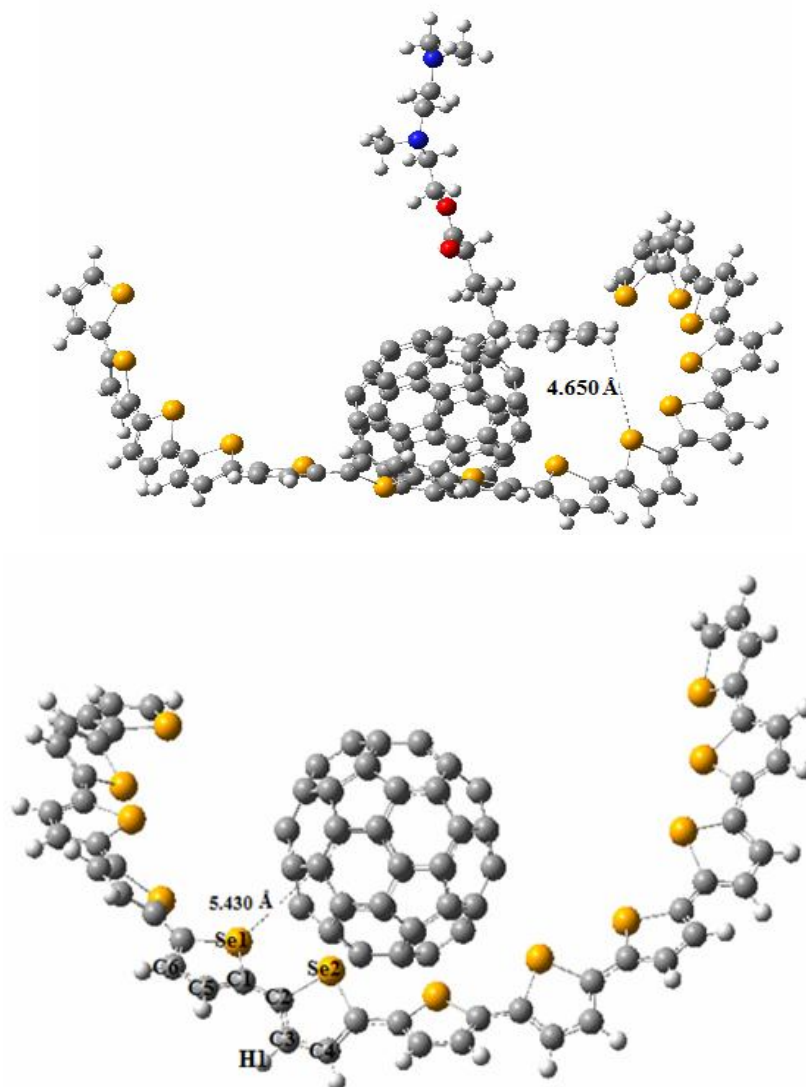


**Fig. 2.** Optimized geometries of (OS)<sub>n=14</sub>/PCBDAN, (OS)<sub>n=14</sub>/PC<sub>60</sub>BM, (OS)<sub>n=12</sub>/C<sub>60</sub>, (OS)<sub>n=14</sub>/C<sub>70</sub>, (OS)<sub>n=14</sub>/C<sub>60</sub> blends.

$$E_{ads} = E_{def} + E_{int} \quad (1)$$

$$E_{int} = E_{(complex)} - (E_{(fullerene\ in\ complex)} + E_{(oligomer\ in\ complex)}) \quad (2)$$

$$E_{def} = E_{(def\ fullerene)} + E_{(def\ oligomer)} \quad (3)$$

$$E_{(def\ fullerene)} = E_{(fullerene\ in\ complex)} - E_{(free\ fullerene)} \quad (4)$$

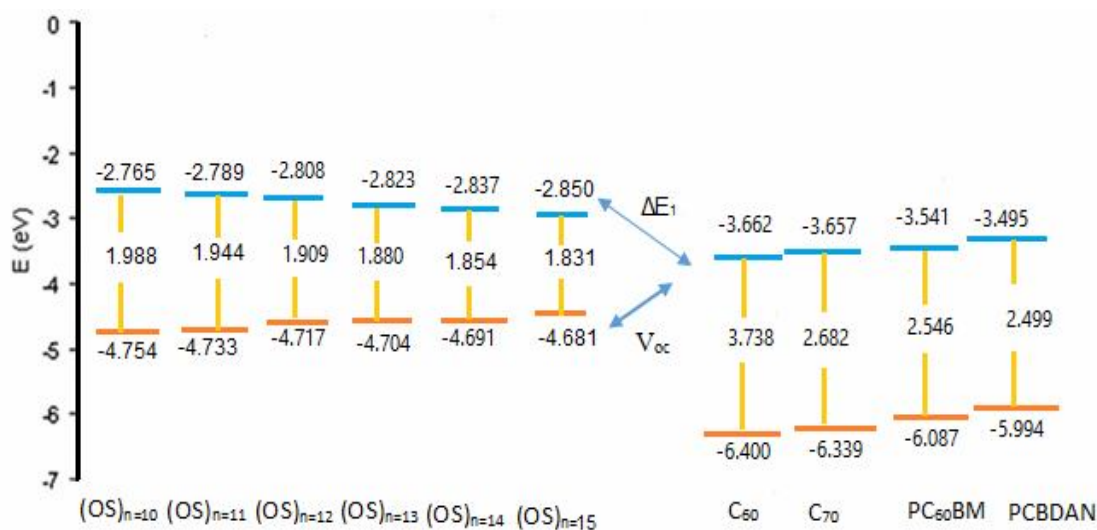
$$E_{(def\ oligomer)} = E_{(oligomer\ in\ complex)} - E_{(free\ oligomer)} \quad (5)$$

A negative value of interaction energy indicates the stability of the studied system. In comparison, the binding energy values of (OS)

C<sub>60</sub> and (OS)<sub>n=14</sub>/C<sub>60</sub> show that the structure with longer oligomer is more stable, which means the (OS)<sub>n=14</sub>/C<sub>60</sub> blend is more stable than the others. According to the values summarized in Table 1, the interaction energy contribution in the complex formation process are obtained large and negative values, that proves the deformation in the direction sustainability is taking place. Among all cases, (OS)<sub>n=14</sub>/C<sub>60</sub>

**Table 1.** Deformation Energy ( $E_{\text{def}}$ ), Interaction Energy ( $E_{\text{int}}$ ), Adsorption Energy ( $E_{\text{ads}}$ ) of  $(\text{OS})_n/\text{Fullerene}$  with the B3LYP/6-311G(d) Method

	$E_{\text{def}}$ (kJ mol <sup>-1</sup> )	$E_{\text{int}}$ (kJ mol <sup>-1</sup> )	$E_{\text{ads}}$ (kJ mol <sup>-1</sup> )
$(\text{OS})_{n=12}/\text{C}_{60}$	-28.701	-0.798	-29.499
$(\text{OS})_{n=14}/\text{C}_{60}$	-33.020	-1.974	-34.994
$(\text{OS})_{n=14}/\text{C}_{70}$	-31.766	-1.040	-32.806
$(\text{OS})_{n=14}/\text{PC}_{60}\text{BM}$	-30.894	-3.393	-34.287
$(\text{OS})_{n=14}/\text{PCBDAN}$	-29.032	-1.782	-30.814

**Fig. 3.** Frontier molecular orbital energy levels of  $(\text{OS})_{n=10-15}$  and  $\text{C}_{60}$ ,  $\text{C}_{70}$ ,  $\text{PC}_{60}\text{BM}$ ,  $\text{PCBDAN}$ .  $V_{\text{oc}}$  is open-circuit voltages  $\Delta E_1$  is energy driving force  $\Delta E_1$  for exciton dissociation.

and  $(\text{OS})_{n=14}/\text{PC}_{60}\text{BM}$  blends have the largest deformation energy and interaction energy. Furthermore, due to the calculated  $E_{\text{ads}}$  values, the complex formation of all complexes is favorable and is in the  $(\text{OS})_{n=14}/\text{C}_{60} >$ ,  $(\text{OS})_{n=14}/\text{PC}_{60}\text{BM} >$   $(\text{OS})_{n=14}/\text{C}_{70} >$   $(\text{OS})_{n=14}/\text{PCBDAN} >$   $(\text{OS})_{n=12}/\text{C}_{60}$  trend.

### Frontier Molecular Orbital

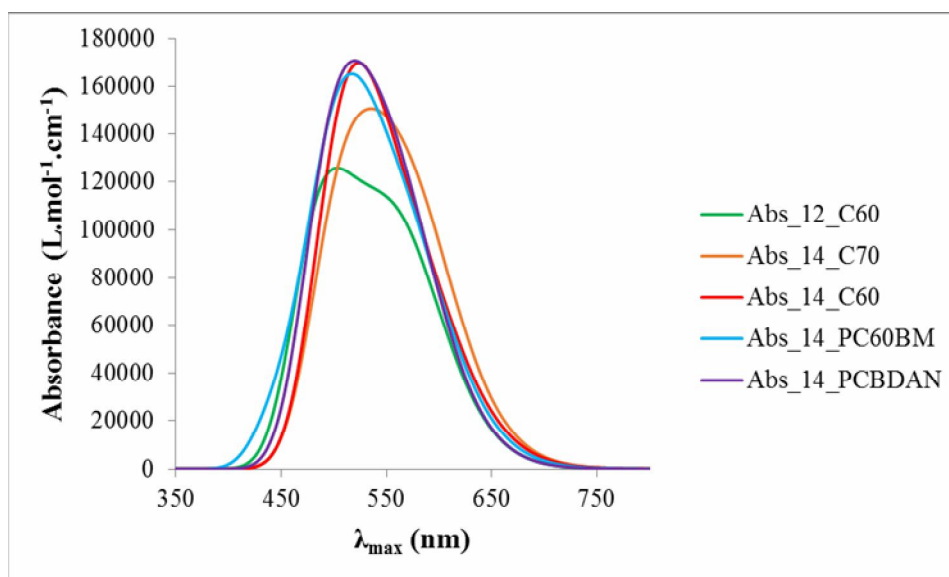
In organic solar cells, frontier molecular orbital energy

levels have a close relation with open-circuit voltages ( $V_{\text{oc}}$ ) and energy driving force ( $\Delta E_1$ ) for exciton dissociation. Namely, the  $V_{\text{oc}}$  is determined by the difference between the HOMO of the donor and the LUMO of the acceptor, according to the empirical equation summarized by Scharber [49], which can be expressed as below:

$$V_{\text{oc}} = \left(\frac{1}{e}\right) \left( |E_{\text{HOMO}}^{\text{Donor}}| - |E_{\text{LUMO}}^{\text{Acceptor}}| \right) - 0.3 \quad (6)$$

**Table 2.**  $\Delta E_{LL}$  &  $V_{OC}$  of  $(OS)_n$ /Fullerene Calculated at B3LYP/6-311G(d) Level of Theory

	$\Delta E_1$ (LUMO <sub>(D)</sub> - LUMO <sub>(A)</sub> ) (eV)	$V_{OC}$ (V)
$(OS)_{n=12}/C_{60}$	0.854	1.055
$(OS)_{n=14}/C_{60}$	0.825	1.029
$(OS)_{n=14}/C_{70}$	0.820	1.034
$(OS)_{n=14}/PC_{60}BM$	0.704	1.150
$(OS)_{n=14}/PCBDAM$	0.658	1.196

**Fig. 4.** Simulated absorption spectra of  $(OS)_{n=14}/PCBDAN$ ,  $(OS)_{n=14}/PC_{60}BM$ ,  $(OS)_{n=12}/C_{60}$ ,  $(OS)_{n=14}/C_{70}$ ,  $(OS)_{n=14}/C_{60}$  blends.

here,  $e$  is the elementary charge, and the value of 0.3 is an empirical factor. The energy difference  $\Delta E_1$  between the LUMOs of the donor and the acceptor should be larger than 0.3 eV, which guarantees efficient exciton split and charge dissociation at the donor/acceptor (D/A) interface. To explore these relationships, the frontier molecular orbital (FMO) energies of all studied acceptors concerning the electron donors  $(OS)_{n=10-15}$  were depicted in Fig. 3. The values of  $\Delta E_1$  and  $V_{oc}$  parameters are reported in Table 2.

The results show that the most favorable value of  $\Delta E_1$  is related to the  $(OS)_{n=14}/PCBDAN$  blend, because of the LUMO orbitals energy levels are located nearly to each other; hence, this complex has the lowest  $\Delta E_1$  and highest  $V_{oc}$  compared to all other complexes. As we know, with increasing the  $V_{oc}$ , the power conversion efficiency (PCE) of the blend is also increased; therefore the  $(OS)_{n=14}/PCBDAN$  blend has higher PCE than other investigated blends.

**Table 3.** Calculated HOMO, LUMO Energies, Electronic & Optical Energy Gap and Exciton Binding Energy of (OS)<sub>n</sub>/Fullerene with the B3LYP/6-311G(d) Method

	HOMO (eV)	LUMO (eV)	E <sub>g,ele</sub> (eV)	E <sub>g,optic</sub> (eV)	E <sub>ex</sub> (eV)
(OS) <sub>n=14</sub> /C <sub>60</sub>	-5.042	-3.516	1.526	1.264	0.262
(OS) <sub>n=12</sub> /C <sub>60</sub>	-5.069	-3.542	1.527	1.268	0.259
(OS) <sub>n=14</sub> /C <sub>70</sub>	-5.058	-3.514	1.544	1.288	0.256
(OS) <sub>n=14</sub> /PC <sub>60</sub> BM	-5.079	-3.396	1.683	1.419	0.264
(OS) <sub>n=14</sub> /PCBDAN	-5.081	-3.361	1.720	1.459	0.261

**Table 4.** Calculated PCE Values of (OS)<sub>n</sub>/Fullerene with the B3LYP/6-311G(d) Method

Power conversion efficiency (PCE)	
C <sub>60</sub> /(OS) <sub>n=12</sub>	7.7%
C <sub>60</sub> /(OS) <sub>n=14</sub>	8.0%
C <sub>70</sub> /(OS) <sub>n=14</sub>	8.2%
PC <sub>60</sub> BM/(OS) <sub>n=14</sub>	9.3%
PCBDAN/(OS) <sub>n=14</sub>	9.7%

### Absorption Spectra

To gain insight into the properties of excited states, the 40 lowest vertical singlet-singlet electronic transition energies and optical absorption spectra of all (OS)<sub>n</sub>/fullerene blends were investigated. Based on the relaxed geometry of entitled blends, the TD-DFT calculations were done at the B3LYP/6-311G(d) level of theory. Figure 4 shows the simulated absorption spectra along with the absorption wavelength. The absorption spectra of all blends show only an extreme peak. The main transitions of all blends occurred in the visible range. The difference in chain length oligomers in the (OS)<sub>n=14</sub>/C<sub>60</sub> and (OS)<sub>n=12</sub>/C<sub>60</sub> blends has led to the hyperchromic effect. This effect defined as an increase in absorptivity at a particular wavelength of light by a solution or substance due to structural changes in a

donor molecule. Comparing the absorption spectrum of blends with its absorption spectrum components, show that the intensity and width of each absorption spectrum are changed with (OS)<sub>n</sub> > (OS)<sub>n</sub>/fullerene > fullerene trends. The Calculated HOMO, LUMO energies, electronic and optical energy gap, and exciton binding energy of (OS)<sub>n</sub>/fullerene complexes are summarized in Table 3.

To estimate the power conversion efficiency (PEC) of the designed blends, we used the Scharber diagrams to predict PCEs (%) of the solar cell combining (OS)<sub>n=14</sub> donor and C<sub>60</sub>, C<sub>70</sub>, PCBM, and PCBDAN. By using the design rules proposed by Scharber *et al.* [29,49] which assumes a fill factor (FF) of 0.75 (we cannot predict the fill factor of 0.75 from the first principles, and in real organic solar cells, the assumed FF is so large that it is usually difficult to

achieve), one can predict the overall PCEs from the band gaps and the LUMO energy levels of the donors. The predicted PCEs of formed blends using the calculated results of  $E_g$  and LUMO energy levels and Sharber diagram are shown in Table 4. As shown, the  $(OS)_{n=14}/PCBDAN$  blend has the highest PCE (with 9.7% value) than the other blends. According to the calculated PCE values, the following trends is seen:  $C_{60}/(OS)_{n=12} < (OS)_{n=14}/C_{60} < (OS)_{n=14}/C_{70} < (OS)_{n=14}/PC_{60}BM < (OS)_{n=14}/PCBDAN$ .

## CONCLUSIONS

The details of structural, electronic, and optical properties of a series of oligoselenophene/fullerene ( $(OS)_n$ /fullerene) blends have been investigated using DFT and TD-DFT methods. The B3LYP/6-311G(d) level of theory was used to consider the electronic and optical features. The HOMO-LUMO energy levels, electronic band gap ( $E_{g,ele}$ ), optical band gap ( $E_{opt}$ ), UV-Vis absorption spectrum, and maximum wavelength ( $\lambda_{max}$ ) of entitled compounds are considered. Due to the calculated  $E_{ads}$  values, the complex formation of all studied blends is favorable and is in the  $(OS)_{n=14}/C_{60} > (OS)_{n=14}/PC_{60}BM > (OS)_{n=14}/C_{70} > (OS)_{n=14}/PCBDAN > (OS)_{n=12}/C_{60}$  trend. Furthermore, results show that the width of the absorption spectrum of all investigated blends are in the range of 400-700 nm and the maximum wavelength in the range of 516.65-536.03 nm. The highest open-circuit voltage ( $V_{OC}$ ) is related to the  $(OS)_{n=14}/PCBDAN$  blend, which indicates that the  $(OS)_{n=14}/PCBDAN$  blend has highest PCE (with 9.7% value) than the other blends.

## ACKNOWLEDGMENTS

The authors thank the Shahid Chamran University of Ahvaz for their support of this scientific research. Also, we are grateful to the Research Council of Shahid Chamran University of Ahvaz for financial support (GN 1397).

## REFERENCES

- [1] Y. Wang, W. Wei, X. Liu, Y. Gu, *Sol. Energy Mater. Sol. Cells* 98 (2012) 129.
- [2] Y. Li, T. Pullerits, M. Zhao, M. Sun, *J. Phys. Chem. C* 115 (2011) 21865.
- [3] E. Bundgaard, F.C. Krebs, *Sol. Energy Mater. Sol. Cells* 91 (2007) 954.
- [4] S. Xiao, A.C. Stuart, S. Liu, W. You, *Appl. Mater. Interfaces* 1 (2009) 1613.
- [5] S. Gunes, D. Baran, G. Gunbas, A. Durmus, A. Fuchsbaue, N.S. Saricifci, L. Toppare, *Polym. Chem. I* (2010) 1245.
- [6] T.A. Skotheim, R.L. Elsenbaumer, J.R. Reynolds, *Handbook of Conducting Polymers*, ed., Marcel Dekker, Inc., New York, 1998.
- [7] C.N. Hoth, P. Schilinsky, S.A. Choulis, C.J. Brabec, *Nano Lett.* 8 (2008) 2806.
- [8] S. Tang, J. Zhang, *J. Phys. Chem. A* 115 (2011) 5184.
- [9] C.J. Brabec, V. Dyakonov, J. Parisi, N.S. Saricifci, *Organic Photovoltaics: Concepts and Realizations*, Springer-Verlag Berlin Heidelberg, New York, 2003.
- [10] R.H. Bube, *Photovoltaic Materials*, Imperial College Press, London, 1998.
- [11] Y. Yi, V. Coropceanu, J.L. Bredas, *J. Am. Chem. Soc.* 131 (2009) 15777.
- [12] B.C. Thompson, J.M.J. Frchet, *Angew. Chem. Int. Ed.* 47 (2008) 58.
- [13] W.C.H. Choy (Ed.), *Organic Solar Cells*, Green Energy and Technology, Springer-Verlag London, 2013.
- [14] X. Song, W. Hua, Y. Ma, C. Wang, Y. Luo, *J. Phys. Chem. C* 116 (2012) 23938.
- [15] C. Risko, M.D. McGehee, J.-L. Bredas, *Chem. Sci.* 2 (2011) 1200.
- [16] J.J.M. Halls, C.A. Walsh, N.C. Greenham, E.A. Marseglia, R.H. Friend, S.C. Moratti, A.B. Holmes, *Nature* 376 (1995) 498.
- [17] G. Dennler, M.C. Scharber, C.J. Brabec, *Adv. Mater.* 21 (2009) 1323.
- [18] G. Yu, J. Gao, J.C. Hummelen, F. Wudl, A.J. Heeger, *Science* 270 (1995) 1789.
- [19] C. Leng, H. Qin, Y. Si, Y. Zhao, *J. Phys. Chem. C* 118 (2014) 1843.
- [20] J.W. Chen, Y. Cao, *Acc. Chem. Res.* 42 (2009) 1709.
- [21] J.Y. Kim, K. Lee, N.E. Coates, D. Moses, T.Q. Nguyen, M.C. Dante, A.J. Heeger, *Science* 317 (2007) 222.
- [22] Y. Liang, Z. Xu, J. Xia, S.-T. Tsa, T. Wu, G. Li, C.



- Ray, L. Yu, *Adv. Mater.* 22 (2010) E135.
- [23] C.J. Brabec, N.S. Sariciftci, J.C. Hummelen, *Adv. Funct. Mater.* 11 (2001) 15.
- [24] Y. He, Y. Li, *Phys. Chem. Chem. Phys.* 13 (2011) 1970.
- [25] Z.-L. Guan, J.B. Kim, H. Wang, C. Jaye, D.A. Fischer, Y.-L. Loo, A. Kahn, *Org. Electron.* 11 (2010) 1779.
- [26] N.-K. Persson, M. Sun, P. Kjellberg, T. Pullerits, O. Inganäs, *J. Chem. Phys.* 123 (2005) 204718.
- [27] Z. MahdaviFar, H. Salmanizadeh, *J. Photochem. Photobiol. A: Chem.* 310 (2015) 9.
- [28] X. Gong, M. Tong, Y. Xia, W. Cai, J. Moon, Y. Cao, G. Yu, C. Shieh, B. Nilsson, A.J. Heeger, *Science* 325 (2009) 1665.
- [29] M.C. Scharber, D. Muehler, M. Koppe, P. Denk, A.J. Heeger, C. Waldauf, C.J. Brabec, *J. Adv. Mater.* 18 (2006) 789.
- [30] C. Winder, G. Matt, J.C. Hummelen, R.A.J. Janssen, N.S. Sariciftci, C. Brabec, *Thin Solid Films* 373 (2002) 403.
- [31] O.M. Sarhangi, S.M. Hashemianzadeh, M.M. Waskasi, A.P. Harzandi, *J. Photochem. Photobiol. A* 225 (2011) 95.
- [32] E.E. Havinga, W. ten Hoeve, H. Wynberg, *Synth. Met.* 299 (1993) 55.
- [33] M.C.R. Delgado, V. Hernandez, J.T.L. Navarrete, S. Tanaka, Y. Yamashita, *J. Phys. Chem. B* 108 (2004) 2516.
- [34] L.J.A. Koster, V.D. Mihailetschi, P.W.M. Blom, *Appl. Phys. Lett.* 88 (2006) 093511.
- [35] A. Ostovan, Z. MahdaviFar, M. Bamdad, *Polymer* 126 (2017) 162.
- [36] Z. MahdaviFar, S. Tajdinin, E. Shakerzadeh, *Appl. Organomet. Chem.* 33 (2019) e4962.
- [37] A. Patra, M. Bendikov, S. Chand, *Acc. Chem. Res.* 4 (2014) 1465.
- [38] A. Patra, M. Bendikov, *J. Mater. Chem.* 20 (2010) 422.
- [39] O. Gidron, Y. Diskin-Posner, M. Bendikov, *J. Am. Chem. Soc.* 132 (2010) 2148.
- [40] A.M. Ballantyne, L. Chen, J. Nelson, D.D.C. Bradley, Y. Astuti, A. Maurano, C.G. Shuttle, J.R. Durrant, M. Heeney, W. Duffy, I. McCulloch, *Adv. Mater.* 19 (2007) 4544.
- [41] a) A.A. Jahnke, B. Djukic, T.M. McCormick, E.B. Domingo, C. Hellmann, Y. Lee, D.S. Seferos, *J. Am. Chem. Soc.* 135 (2013) 951.
- [42] A. Botta, C. Costabile, V. Venditto, S. Pragliola, R. Liguori, A. Rubino, D. Alberga, M. Savarese, C. Adamo, *J. Polym. Sci., A: Polym. Chem.* 55 (2018) 242.
- [43] R. Kroon, A. Melianas, W. Zhuang, J. Bergqvist, A.D. Z Mendaza, T.T. Steckler, L. Yu, S.J. Bradley, C. Musumeci, D. Gedefaw, T. Nann, A. Amassian, C. Müller, O. Inganäs, M.R. Andersson, *Polym. Chem.* 6 (2015) 7402.
- [44] K.A. Mazzio, M. Yuan, K. Okamoto, C.K. Luscombe, *ACS Appl. Mater. Interfaces* 3 (2011) 271.
- [45] M.J. Frisch, G.W. Trucks, H.B. Schlegel, G.E. Scuseria, M.A. Robb, J.R. Cheeseman, G. Scalmani, V. Barone, B. Mennucci, G.A. Petersson, H. Nakatsuji, M. Caricato, X. Li, H.P. Hratchian, A.F. Izmaylov, J. Bloino, G. Zheng, J.L. Sonnenberg, M. Hada, M. Ehara, K. Toyota, R. Fukuda, J. Hasegawa, M. Ishida, T. Nakajima, Y. Honda, O. Kitao, H. Nakai, T. Vreven, J.A. Montgomery, Jr., J.E. Peralta, F. Ogliaro, M. Bearpark, J.J. Heyd, E. Brothers, K.N. Kudin, V.N. Staroverov, R. Kobayashi, J. Normand, K. Raghavachari, A. Rendell, J.C. Burant, S.S. Iyengar, J. Tomasi, M. Cossi, N. Rega, J.M. Millam, M. Klene, J.E. Knox, J.B. Cross, V. Bakken, C. Adamo, J. Jaramillo, R. Gomperts, R.E. Stratmann, O. Yazyev, A.J. Austin, R. Cammi, C. Pomelli, J.W. Ochterski, R.L. Martin, K. Morokuma, V.G. Zakrzewski, G.A. Voth, P. Salvador, J.J. Dannenberg, S. Dapprich, A.D. Daniels, Ö. Farkas, J.B. Foresman, J.V. Ortiz, J. Cioslowski, D.J. Fox, *Gaussian 09* (Gaussian, Inc., Wallingford CT, 2009).
- [46] S.S. Zade, M. Bendikov, *Org. Lett.* 8 (2006) 5243.
- [47] R. Bauernschmitt, R. Ahlrichs, *Chem. Phys. Lett.* 256 (1996) 454.
- [48] R.E. Stratmann, G.E. Scuseria, M.J. Frisch, *J. Chem. Phys.* 109 (1998) 8218.
- [49] M.C. Scharber, N.S. Sariciftci, *Prog. Polym. Sci.* 38 (2013) 1929.